

## LATTICE AND BEAM DYNAMICS (WBS 1.11)

The collider is composed of two identical non-circular concentric rings in a common horizontal plane, oriented to intersect with one another at six crossing points. Each ring consists of three inner arcs and three outer arcs and six insertions joining the inner and outer arcs. Each arc is composed of 11 FODO cells. The insertion has nine quadrupoles and six dipoles (four for dispersion matching and two for the beam crossing) on each side of the crossing point. A general layout of the collider ring is shown on Fig. 11-1.

In the current lattice version RHIC 92 Rev. 0.5, the insertion is tunable from  $\beta^* = 1$  m to  $\beta^* = 10$  m and beyond. The curves for the gradients versus  $\beta^*$  are smooth and continuous. Furthermore, the crossing point  $\beta^*$  is variable at different betatron tunes ranging from  $\nu_{H,V} = 27.823$  to 29.195. The selected operating point will be at  $\nu_H = 28.19$  and  $\nu_V = 29.18$ .

The ring structure conforms closely to the geometry of the existing tunnel. In the standard configuration, there is reflection symmetry with respect to each arc bisector. The polarity sequence of all quadrupoles is anti-symmetric with respect to the crossing points. This gives rise to three superperiods, with one sextant consisting of an inner arc plus insertion and its neighboring sextant consisting of an outer arc plus insertion as the fundamental period. The superperiodicity will be reduced if the insertions are not all identically tuned, e.g., in order to provide different crossing point conditions (crossing angles, beta values, detector magnets). On the other hand, machine functions, such as beam injection and beam abort, can be accommodated by the standard insertion. It is expected that the collider will initially be operated in its simplest configuration, i.e., one with the highest possible superperiodicity and  $\beta^* = 10$  m, and that departure from this configuration will be introduced as operational experience grows.

It proved to be too expensive to place the transition energy outside the operating range from 10 - 100 GeV/u, so that the heavy ion beams will have to be accelerated through transition. Stored beam operation near the transition energy is not possible; this leaves a small gap in the operating range for beam energies very close to the nominal  $\gamma_T = 22.89$ .

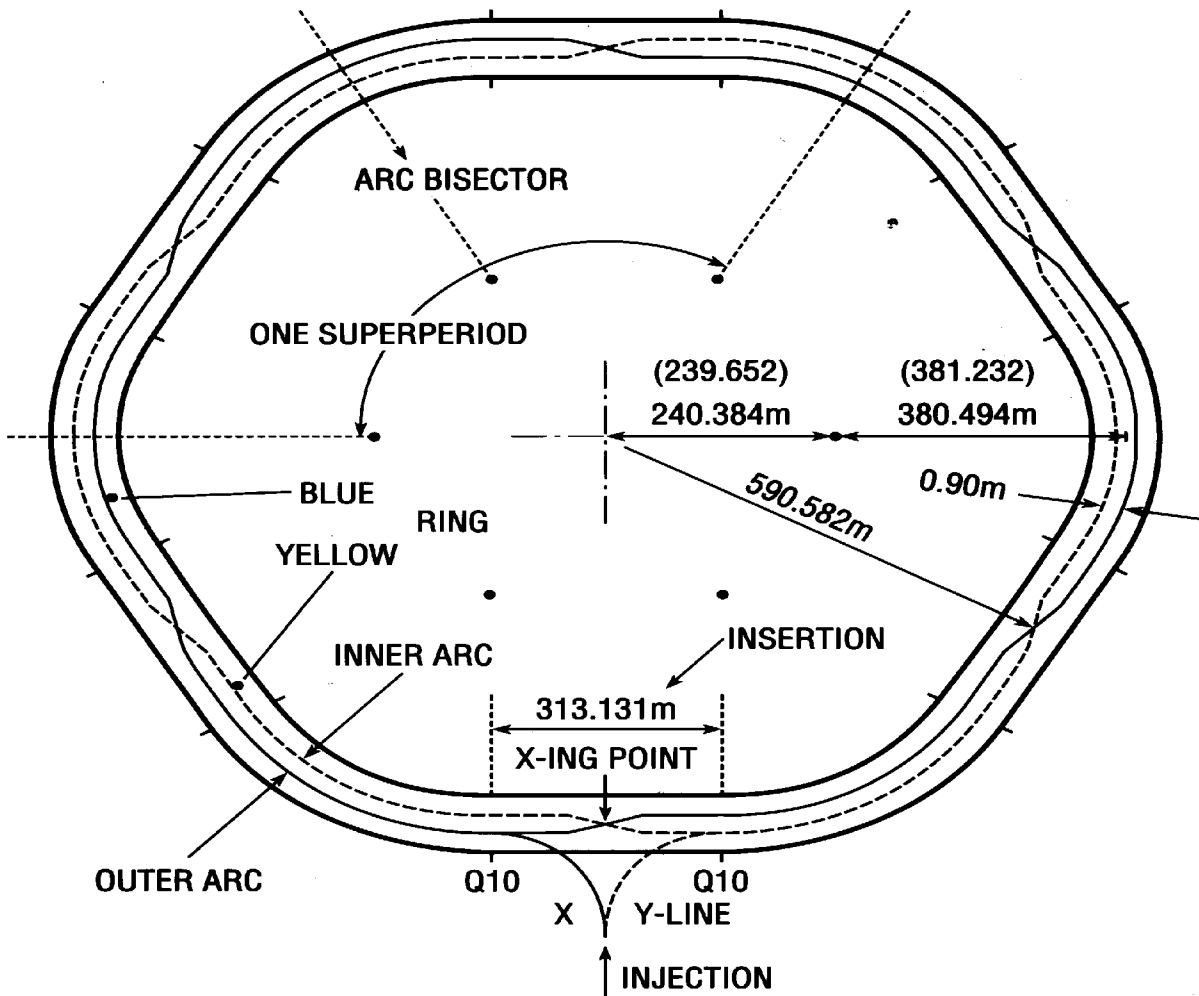


**Fig. 11-1.** Layout of the collider and in parenthesis of the tunnel.  
The ring circumference is 3833.845 m.

### i. Arcs

The choice of the arc structure has a profound impact on the performance and the cost of the collider. Intrabeam scattering in the case of heavy ions results in larger longitudinal and transverse emittances and thus larger aperture requirements relative to a proton accelerator. The desire to keep the aperture requirements small points to a lattice solution with stronger focusing and higher transition energy. On the other hand, the requirements of the chromaticity sextupole system, the rf requirements at low energies, the desire to avoid passage through transition with protons, and quadrupole cost considerations favor weaker focusing and limit the transition energy to below the AGS energy. These arguments lead to the adoption of a solution with 11 FODO arc cells per sextant, with a transition energy of  $\gamma_T = 22.89$  and a tune  $\nu_H = 28.19$  and  $\nu_V = 29.18$ . The half cell geometry is shown in Fig. 11-2. Each cell is  $\sim 29.622$  m long; it deflects the beam by  $\sim 77.85$  mrad and has a betatron phase advance which varies from  $\mu_H = 80.55^\circ$  and  $\mu_V = 85.40^\circ$  to  $\mu_H = 82.42^\circ$  and  $\mu_V = 87.25^\circ$  with  $\beta^* = 10$  to 1 m respectively. The cell betatron and dispersion functions are shown in Fig. 11-3, and the principal characteristics are tabulated in Table 11-1.

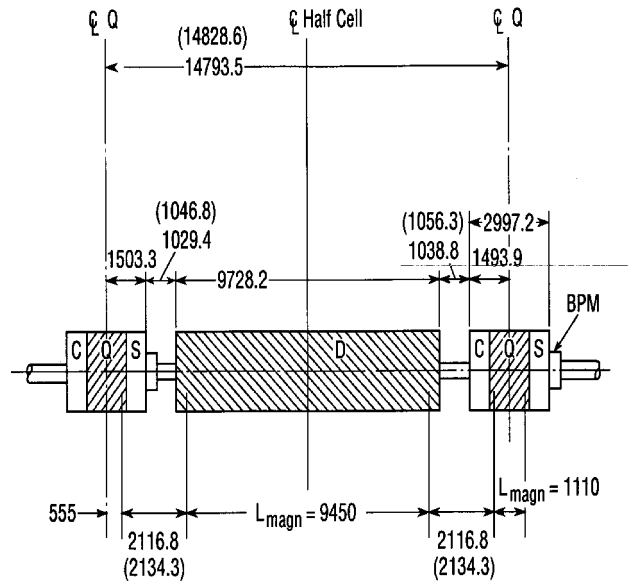


**Fig. 11-2.** Layout of inner(outer) arc half cell. (Dimensions in mm.)

**Table 11-1.** Principal Characteristics of Arc Cell

	Inner Arc	Outer Arc
Length (m)	29.5871	29.6571
Deflection Angle (mrad)		77.8481
Average Radius of Curvature (m)*	380.0443	380.9443
Dipole Bending Radius (m)		242.7806
Distance between Centerlines (m)		0.9000
Dipole Strength $\int B d\ell/B\rho$		0.038924
Quadrupole Strength (all insertions at $\beta^* = 10$ m)		
$\int B' d\ell/B\rho, (m^{-1})$ F&D		0.09020 & 0.09320
Betatron Phase Advance (all insertions at $\beta^* = 10$ m)		
$\Delta\mu_H/2\pi, \Delta\mu_V/2\pi$	0.2234 & 0.2369	0.2241 & 0.2376
$\hat{\beta}_H$ & $\check{\beta}_H$ in quadrupole midplanes (m)	49.71 & 10.56	49.84 & 10.53
$\hat{\beta}_V$ & $\check{\beta}_V$	48.55 & 9.82	48.70 & 9.79
$\hat{X}_p$ & $\check{X}_p$ in quadrupole midplanes (m)	1.841 & 0.939	1.837 & 0.936
$\chi_{H,V} = \Delta v/(\Delta p/p)$	-0.273 & -0.284	-0.275 & -0.286

\*Defined by quad centers

The inner and outer arcs are constructed with the same magnet types and are identical, except for the small difference in average radii, obtained from adjustments in the drift space lengths. The inner and outer arcs of a magnet sextant are concentric. The quadrupole center-to-center distance between two rings is chosen to be 90 cm so that each ring line can be housed in a separate vacuum vessel. There are eleven identical cells in each arc, each with two quadrupoles and two dipoles, resulting in a count of 132 arc dipoles and 138 arc quadrupoles per ring (since Q10 must be double counted). Note, however, that D8 is identical to the arc dipole, resulting in a count of 144 arc-size dipoles.

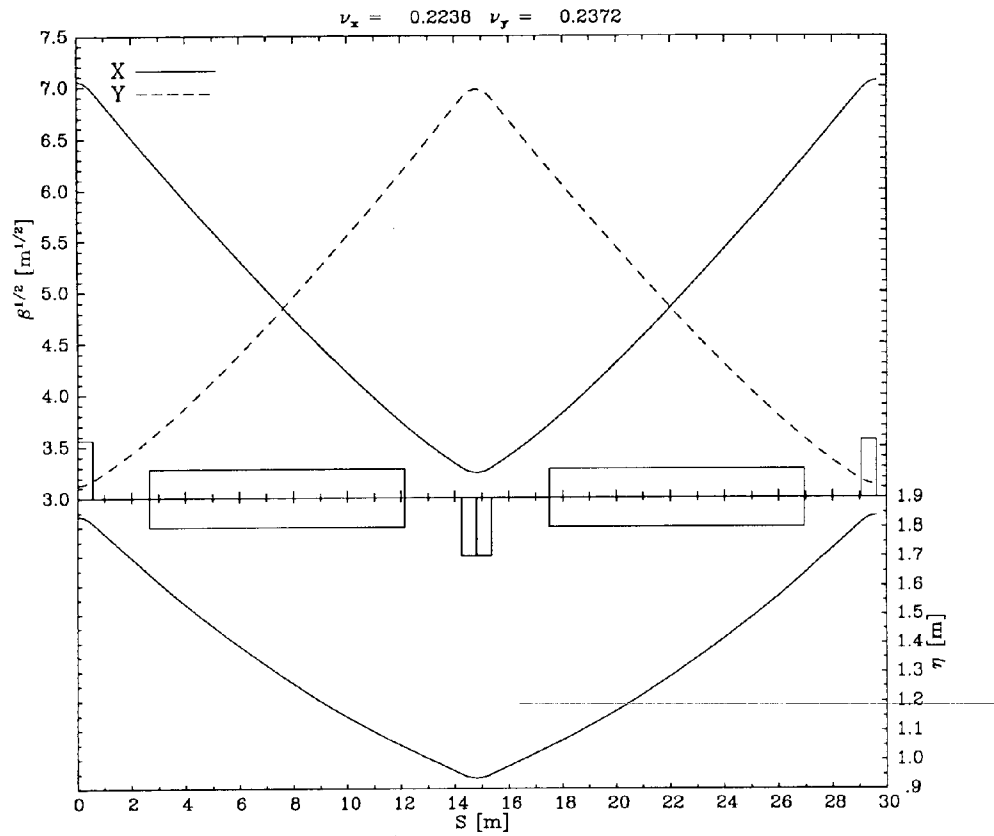


**Fig. 11-3.**  $\beta$  and  $X_p$  functions of RHIC regular arc cell for  $\beta$ .